ACS OMEGA

http://pubs.acs.org/journal/acsodf

Article

Experimental Hydrate Phase Equilibrium Data Relevant to Bitter Melon, Pineapple, and Grape Juice Concentration

Nkululeko Nkosi, Diakanua Nkazi, and Kaniki Tumba*

Cite This: *ACS Omega* 2022, 7, 34741−34751

Read Online

ACCESS | Metrics & More | Article Recommendations

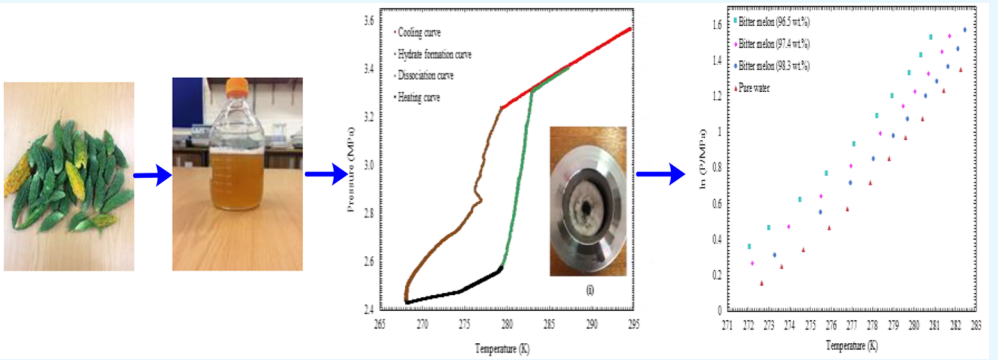

ABSTRACT: One of the major challenges experienced by the fruit juice industry is the steady rise in energy costs. Hence, it is of industrial interest to find possible environmentally friendly measures that reduce energy consumption while cost-effectively maintaining the quality of manufactured products. Hydrate-based juice concentration technology can be used to overcome this challenge. In the present work, experimental hydrate phase equilibrium conditions of three systems involving juices (system 1, CO_2 + grape juice; system 2, CO_2 + pineapple juice; system 3, CO_2 + bitter melon juice) were measured using an isochoric pressure search method. The temperature and pressure ranges for reported experimental data were 272.6−282.3 K and 1.17−3.85 MPa, respectively. Results have shown that a decrease in water cut from 98.3 to 88.5 ± 2.53 wt % could shift the hydrate phase equilibrium conditions toward higher pressures and lower temperatures. This proved that all investigated juices exhibited inhibitory effects on gas hydrate formation. To properly assess the energy requirements for this novel technology, molar hydrate dissociation enthalpies were estimated using the Clausius−Clapeyron relations under different measurement conditions. Finally, it was established that a hydrate-based fruit juice concentration technology would be a credible alternative to existing commercial technologies, on the basis of the dehydration ratio of 57% obtained in the present study.

1. INTRODUCTION

There is a continuous energy demand, which has led to the increased use of available fossil fuels due to rapidly increasing population, enhanced living standards, and expansion of industrial activities.[1] This, in turn, has placed pressure on existing fossil fuels, leading to significant exhaustion of their reserves and increased ecological repercussions. However, despite this, it has become impossible to increase fossil fuel use due to the imposed environmental legislation and the 2050 targets set by United Nations for a net-zero carbon emission.[2−4] As the availability of fossil crude oil experiences a significant decline globally, its economic price has overshadowed its environmental cost.[1] This steep, sharp rise in energy resource prices is due to an increasing global energy demand coming from fast-emerging economies. This nonnegotiable energy resource price from a nonrenewable resource is one of the main drivers for the promotion of renewable energies. Consequently, interest has shifted to carbon-neutral sources of energy or energy-efficient and environmentally friendly chemical processes. In the search for strategies to minimize energy consumption, carbon dioxide hydrate based processes have received increasing attention from numerous industries. The technology has been successfully applied in the desalination of water,[5−8] separation of gases,[9−11] carbon dioxide capture and sequestration,[1,12,13] and preservation processes in the food industry.[14−21] It has been recognized as a cost-effective cold thermal energy storage solution.

As CO_2 hydrate technology becomes a point of attraction in the food industry, the demand for cold thermal energy storage

Received: January 27, 2022
Accepted: March 25, 2022
Published: September 21, 2022

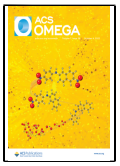

Table 1. CAS Registry Number and Purity of the Chemicals

component	CAS registry no.	supplier	mass fraction	conductivity[b] (μS cm^{-1}) this work	conductivity[b] (μS cm^{-1}) literature[32]	measurement method
water	7732-18-5	authors' laboratory		0.055	0.055	conductivity meter
carbon dioxide	124-38-9	Afrox, South Africa	>0.999[a]			none

[a]Purity provided by Afrox. [b]At 298.15 K.

has rapidly increased.[22−24] This is due to rising health awareness. Hence, there is a high demand globally for natural foods having natural bioactive compounds, and fruit juices are among them. Due to the increased energy requirements, existing conventional concentration processes fail to meet and keep up with the global demand for storage purposes and preservation of fruit juices. Moreover, these processes fail to maintain the quality of products manufactured due to unfavorable changes in nutritional contents. The main factors in these processes' challenges are their reliance on thermal evaporation (180−2160 kJ/kg water), freezing (936−1800 kJ/kg water), and pressure gradient concentration. To mitigate these challenges, the CO_2 hydrate technology offers better energy savings and the preservation of bioactive compounds. This is due to the low temperature requirements and the low hydrate latent heat of fusion (252−360 kJ/kg water). This means that the CO_2 hydrate technology requires milder conditions in comparison to conventional fruit juice concentration processes. Moreover, since CO_2 is considered to be environmentally benign and has been widely used in the food processing industry, the CO_2 hydrate based technology seems to be a gentle, novel technology to concentrate fruit juices.

Before the CO_2 hydrate based technology is applied to the concentration process, there is a need to obtain hydrates (pure water and juices) with time-independent as well as time-dependent properties (structural, transport, and kinetic), including hydrate dissociation conditions. Such properties and equilibrium data can be measured experimentally. These data can be used to test existing thermodynamic models or modify the existing models to estimate the equilibrium conditions for clathrate hydrate forming systems. If such data (i.e., experimental and modeled) are established to be accurate enough, they can subsequently be used as a tool for designing, optimizing, or simulating economically viable and practical hydrate-based industrial processes. To date, gas hydrate technology has been used for the concentration of food substances such as juices[14−19] and coffee.[25] These studies have focused on hydrate phase equilibrium and hydrate formation kinetics measurements.

Huang et al.[15] investigated the use of CH_3Br and CCl_3F as hydrate formers to concentrate orange, apple, and tomato juice. These authors were able to remove about ±80% of the water content from fruits. Despite satisfactory concentration results, gas hydrate formation resulted in the development of a bitter aftertaste and a change in the product color, odor, and flavor.

After more than three decades, Purwanto et al.[26] carried out a study on xenon gas hydrate to concentrate coffee solutions. The authors' objective was to address challenges with hydrate formers reported by Huang and co-workers.[15] They achieved higher concentrations when the stirring speed was increased. However, it was reported that the water removal efficiency at higher temperatures was negatively affected. Despite the authors' promising results, due to the cost and environmental issues related to the xenon hydrate former,[20] a search for alternative hydrate former(s) was suggested.

To date, the use of nitrous oxide (N_2O), nitrogen (N_2), or a rare gas as hydrate formers is known to overcome previously reported problems. However, CO_2 gas hydrate technology has emerged as a novel technology for concentrating fruit juices such as orange, apple, and tomato.[14,17−19,27−29] This technology to concentrate fruit juice was first reported by Li et al.[17] These authors investigated the application of CO_2 hydrate technology to concentrate tomato juice with a maximum dehydration ratio of 63.2% at an initial pressure of 3.95 MPa. Furthermore, Li et al.[14] undertook another study to concentrate orange juice. This study achieved a maximum dehydration ratio of 57% with an initial pressure of 4.1 MPa. Finally, the CO_2 hydrate technology was developed further by Seidl et al.[29] and Claßen et al.[28] to concentrate apple juice. In the study by Seidl et al.,[29] a maximum °Brix value of 27 was achieved, whereas Claßen et al.[28] obtained a °Brix value of 45. The low concentration reported by Seidl et al.[29] is due to the reactor used (bubble column). In all of these studies, the reported hydrate dissociation data indicated a shift to higher pressures and lower temperatures, indicating inhibiting effects. Therefore, it was concluded that the orange, apple, and tomato juice contents acted as inhibitors. This also indicates that hydrate formation in the presence of juices may be leading to increased energy demand. This was supported by an experimental study on the hydrate formation kinetics of orange juice.[18] Longer induction times were observed, rendering the CO_2 hydrate technology impractical for commercialization. Moreover, when the sugar content was considered as a factor in hydrate formation, conflicting results were observed by Safari and Varaminian[18] as well as Andersen and Thomsen.[20] To mitigate these limitations, researchers will have to carry out an optimization study on the phase equilibrium data of juice concentration. Moreover, the characterization of juice contents should be considered. Therefore, more experimental hydrate phase equilibrium data must be made available, considering the previously mentioned challenges.

To the best of our knowledge, there has been limited research devoted to the study of hydrate-based juice concentration as an alternative to evaporation. Moreover, no studies have focused on hydrate dissociation conditions using carbon dioxide and bitter melon or grape or pineapple juice systems under different water cuts. The present study investigates the CO_2 hydrate based technology in the juice concentration process. For this purpose, experimental hydrate phase equilibrium conditions of three systems containing juices (system 1, CO_2 + grape juice + water; system 2, CO_2 + pineapple juice + water; system 3, CO_2 + bitter melon juice + water) were considered in the absence and presence of juice with different water cuts ranging from 88.5 to 98.3 ± 2.53 wt % to evaluate the novel concentration technology based on gas hydrate formation. These hydrate dissociation conditions are important and can be simultaneously measured in hydrate

https://doi.org/10.1021/acsomega.2c00551
ACS Omega 2022, 7, 34741−34751

kinetic studies. Due to the lack of accurate information regarding the composition of juices, it was impossible to develop a thermodynamic model to predict and compare with experimental data.

2. EXPERIMENTAL SECTION

2.1. Materials. Materials used for this study include ultrapure Millipore-Q water, fruits, and carbon dioxide (CO_2) gas. Ultrapure Millipore water was obtained in the laboratory of this research group. The CO_2 gas used was of food-grade quality, and it was supplied by Afrox (South Africa). Further details regarding these two chemicals are gathered in Table 1. Raw fruits (grape, pineapple, and bitter melon) were purchased from a Food Lovers supermarket in KwaZulu-Natal (Durban, South Africa). These fruits were carefully squeezed to extract juices freshly, and their typical compositions are listed in Tables 2−4 and are discussed later in the Results and Discussion. An accurate analytical balance, Model AS220/C/2 (supplied by RADWAG, Poland) with an uncertainty of $\pm 1 \times 10^{-7}$ kg in mass was used to prepare juice solutions having an uncertainty level of $\pm 5 \times 10^{-7}$ m^3 gravimetrically.

Table 2. Composition of the Investigated Bitter Melon Juice[c]

proximate	quantity (mean ± SD) (mg/100 g)		
moisture content[a]	96.5 ± 2.53	97.4 ± 2.53	98.3 ± 2.53
total solids[a]	3.5 ± 0.02	2.6 ± 0.02	1.7 ± 0.02
total ash[a]	0.386 ± 0.043	0.307 ± 0.043	0.187 ± 0.043
lipids	2.3 ± 0.01	1.83 ± 0.67	1.21 ± 0.01
pH[b]	4.31 ± 0.01	4.42 ± 0.01	4.47 ± 0.01
ascorbic acid (vitamin C)	68.58 ± 3.16	53.81 ± 3.16	37.3 ± 3.16

[a]Expressed as wt %. [b]Expressed as pH scale. [c]AOAC International.[30]

Table 3. Composition of the Investigated Grape Juice[c]

proximate	quantity (mean ± SD) (mg/100 g)		
moisture content[a]	88.5 ± 2.53	91.4 ± 2.53	94.3 ± 2.53
total solids[a]	11.5 ± 0.02	8.6 ± 0.02	5.7 ± 0.02
total ash[a]	0.263 ± 0.043	0.217 ± 0.043	0.145 ± 0.043
lipids	5.93 ± 0.67	4.78 ± 0.67	3.18 ± 0.01
pH[b]	3.92 ± 0.01	4.42 ± 0.01	4.51 ± 0.01
ascorbic acid (vitamin C)	18.55 ± 0.92	13.45 ± 3.16	10.81 ± 3.16

[a]Expressed as wt %. [b]Expressed as pH scale. [c]AOAC International.[30]

Table 4. Composition of the Investigated Pineapple Juice[c]

proximate	quantity (mean ± SD) (mg/100 g)		
moisture content[a]	91.1 ± 2.53	93.3 ± 2.53	95.6 ± 2.53
total solids[a]	8.9 ± 0.02	6.7 ± 0.02	4.9 ± 0.02
total ash[a]	0.216 ± 0.043	0.168 ± 0.043	0.121 ± 0.043
lipids	7.81 ± 0.01	5.85 ± 0.67	4.69 ± 0.01
pH[b]	3.72 ± 0.01	4.12 ± 0.01	4.44 ± 0.01
ascorbic acid (vitamin C)	15.4 ± 0.87	11.95 ± 3.16	8.58 ± 3.16

[a]Expressed as wt %. [b]Expressed as pH scale. [c]AOAC International.[30]

2.2. Apparatus. In this study, a high-pressure equilibrium cell was used. It was made of stainless steel (SS 316L) (supplied by Büchi, Switzerland) with an internal volume of 100 mL. The cell's interior is hydrophobically coated with an alloy (nickel−chromium−iron−molybdenum) and is capable of withstanding temperatures and pressures up to 473.15 K and 10 MPa, respectively. A four-wire Pt-100 thermocouple (supplied by Grant Instruments, United Kingdom), with an uncertainty of ±0.3 K, measured the system and liquid bath temperature. A pressure transducer (supplied by ESI Technology, United Kingdom) having an uncertainty of ±0.25% of the full scale measured the inside pressure of the high-pressure equilibrium cell. A magnetic stirrer bar was with a capacity of 1000 rpm was used to achieve a thermodynamic equilibrium quickly and ensure proper mixing of the contents in the cell. An LTC4 temperature-controlled unit (supplied by Grant Instruments, United Kingdom) consisting of a TX150 Optima circulating bath and an R4 tank/refrigeration unit was used. It allowed us to set and control the system temperature, corresponding to the liquid bath temperature. The coolant was an aqueous solution of glycerol. Any trapped air inside the cell was removed by a vacuum pump (supplied by Gardner Denver, United States). The apparatus was connected to an SQ2020-1F8 data acquisition unit (supplied by Grant Instruments, United Kingdom) and interfaced with a computer to monitor pressure and temperature data at particular intervals using SquirrelView software. An overall schematic diagram of the experimental setup used in this study is illustrated in Figure 1.

2.3. Sample Preparation. Samples were prepared using a 500 cm^3 volumetric flask. First, the flask was thoroughly washed and rinsed with distilled water. Then, different concentrations of fruit juices were configured using freshly produced ultrapure Millipore water. An accurate analytical balance was used to prepare juice solutions having an uncertainty level of ±0.5 cm^3 gravimetrically. These concentrations were prepared by placing the desired amount of ultrapure Millipore water in a 500 cm^3 volumetric flask containing fruit juice. Freshly prepared samples were kept in an ultrasonic bath for 15 min. Finally, pure and dilute fruit juice samples were stored in the refrigerator and were kept at T = 277.15 K. The compositions of investigated fruit juices, using a well-defined procedure in the literature,[30] is reported in Tables 2−4.

2.4. Experimental Methods. *2.4.1. Hydrate Phase Equilibrium Measurements.* In this study, a pressure-search method (graphical technique), as described by Sloan and Koh[31] and Tumba et al.,[32] and material balance calculations were used to generate experimental hydrate equilibrium data (hydrate−vapor−liquid) for the carbon dioxide hydrate in the presence of bitter melon, grape, or pineapple juice. At the beginning of each experiment, the equilibrium cell was washed with soapy liquid and repeatedly rinsed with ultrapure Millipore water. Once the cell had been adequately cleaned, it was evacuated for approximately 30 min using a vacuum pump. This was to avoid contamination of the cell injection port and help clean the cell. Then, the inlet valve was closed to maintain the cell under vacuum. After the initial evacuation, the appropriate quantity of ultrapure Millipore water or juice sample (approximately 40 cm^3 with an uncertainty level of ±0.5 cm^3) was injected into the equilibrium cell to form hydrates with all of the injected gas. In this study, the assumed molar ratio between gas and ultrapure Millipore water was 1:6

https://doi.org/10.1021/acsomega.2c00551
ACS Omega 2022, 7, 34741−34751

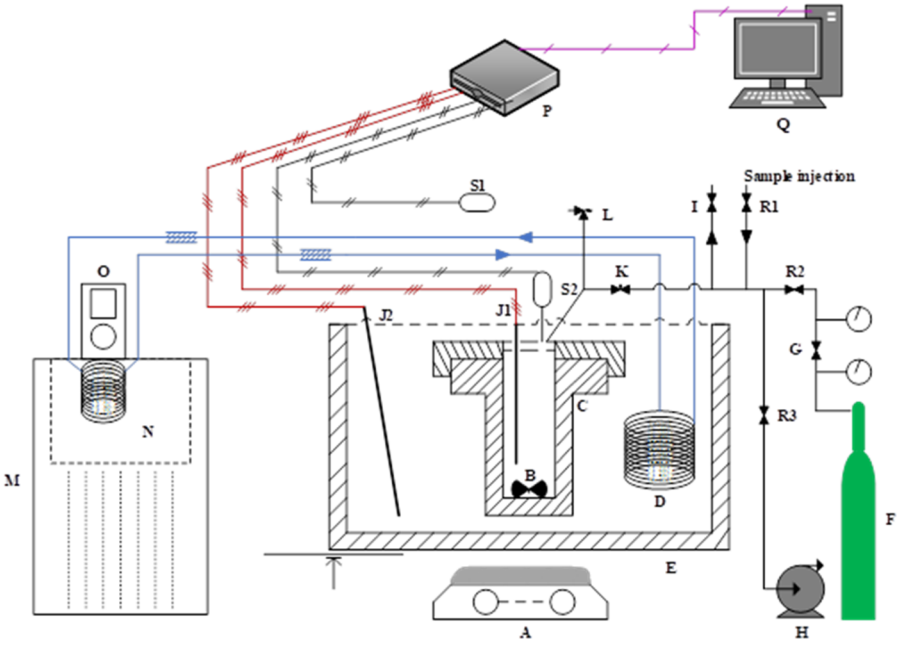

Figure 1. Schematic diagram for the high-pressure equilibrium apparatus: (A) magnetic stirrer; (B) neodymium magnet stir bar; (C) high-pressure equilibrium cell; (D) cooling coil; (E,) thermostated bath; (F) gas cylinder; (G) pressure regulator; (H) vacuum pump; (I) vent valve; (J1,2) temperature probes (Pt-100); (K) needle valve for loading; (L) relief valve; (M) LTC4 unit; (N, LTC4 unit), built-in circulating bath; (O) circulating thermostat; (P) data acquisition system; (Q) computer; (R1−3) shut-off valves; (S1,2) pressure transducers.

in the gas hydrates. Again, the equilibrium cell was evacuated to eliminate any presence of air for 5 min. Afterward, the equilibrium cell was immersed into a temperature-controlled (filled with an equal volume of water and glycerol) liquid bath to cool the equilibrium cell. The system temperature was set at 293.15 K, using a TX150 Optima circulating bath. Then, the cell was pressurized with the hydrate former (CO_2) by increasing the inlet flow, passing it through the pressure-regulated valve until the corresponding operating pressure was reached. After the cell was pressurized, the pressure-regulating valve was closed and the magnetic stirrer was switched on and set at a speed of 500 rpm to agitate the phase inside the equilibrium cell. The liquid phase (ultrapure Millipore water or juice sample) was allowed to stabilize to a temperature of 293.15 K for at least a period of 45−90 min, depending on the liquid sample.

When the system pressure was stabilized and the gas was fully absorbed in water, the data were recorded using SquirrelView software. Then the temperature-controlled liquid bath was set to approximately 283.15 K, below the estimated hydrate dissociation temperature. This process is known as the cooling phase. Two distinct slopes represent this in the cooling curve of Figure 2. The considerable decrease in system pressure categorizes the first slope, the formation of hydrates. This represented the occurrence of the nucleation process. In this process ($P-T$ curve), the pressure is a function of the temperature change, and this is obtainable using the hydrate−vapor−liquid isochoric curve.[31,33] The system pressure was expected to decrease sharply on the second slope. This was observed by a sudden change in gradient on the cooling curve. The observed sharp decrease in the slope indicates hydrate growth within the system. If there was no sharp decrease observed in system pressure, the system was further subcooled by decreasing the liquid bath temperature at a rate of 1.0 K/h until the hydrate/semiclathrate hydrate formation was observed. Cooling was stopped when the system pressure

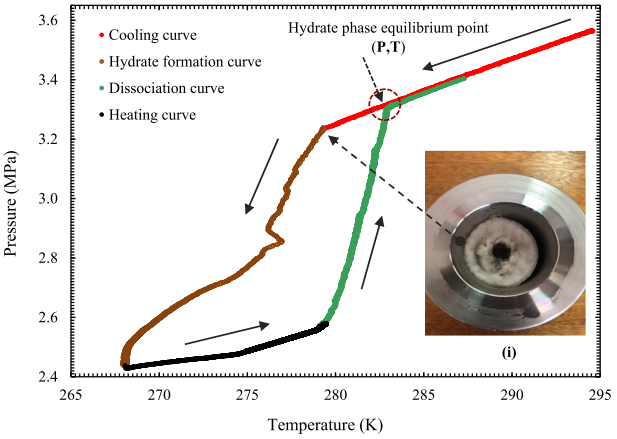

Figure 2. Pressure and temperature trace for the formation and dissociation of a simple hydrate using an isochoric pressure search method (this study). The photograph (inset) taken in this study shows the hydrate that was formed during the experiment.

and temperature were in equilibrium (decay was less than 0.005 MPa/h).

After the hydrate formation by isochoric cooling, the magnetic stirrer was switched off, the system was heated to dissociate the hydrate, the trapped gas was released into the vapor space, and the increment was done in a stepwise manner. Large temperature increments of 2 K/h were initially used until the conditions were closer to those of the dissociation point. From that point on, the temperature was gradually increased by 0.1 K/h until the actual dissociation point was obtained. This point that indicates the intersection determined the equilibrium transition (intersection between cooling and heating curves) from hydrate + liquid + gas to liquid + gas is highly dependent on the heating curves. After the dissociation point, the change in system pressure was a function of

https://doi.org/10.1021/acsomega.2c00551
ACS Omega 2022, 7, 34741−34751

temperature. Then, the system temperature was raised back to 293.15 K.

3. RESULTS AND DISCUSSION

3.1. Hydrate Equilibrium Curve. Since the equipment was new, its reliability and the validity of the experimental procedure had to be examined before generating the hydrate phase equilibrium data reported in this study. The binary test system consisted of carbon dioxide and pure water (CO_2 + H_2O), as intensive studies have already been carried out for this mixture under hydrate-forming conditions. Numerous hydrate data are available in the literature for this system. Eleven gas hydrate dissociation points (P and T), under a liquid water (L_w) + hydrate (H) + CO_2 vapor (V) equilibrium, for the CO_2 + H_2O test system were measured. In addition, the hydrate dissociation data were compared with the literature data of Mooijer-Van Den Heuvel et al.,[34] Smith et al.,[35] and Adisasmito et al.[36] Table 5 and Figure 3 present the experimental data as measured in this study and a graphical view of the same data in the temperature and pressure ranges of 272.6−282.3 K and 1.1703−3.8481 MPa. As shown in Figure 3, there is reasonable agreement between the experimental data and the reported literature data for the carbon dioxide + H_2O test system.

Experimental hydrate phase equilibrium conditions (system 1, CO_2 + grape juice + water; system 2, CO_2 + pineapple juice + water; system 3, CO_2 + bitter melon juice + water) were measured under different water cuts of 96.5, 97.4, and 98.3 ± 2.53 wt %. The water cuts for pure bitter melon, grape, and pineapple juices were 96.5, 88.5, and 91.1 wt % with an uncertainty of ±2.53. Furthermore, these raw juice concentrations are consistent with typical values at the inlet of evaporators. To the best of our knowledge, there are no experimental data for these investigated systems at different fruit juice−water cuts. The measured data are reported in Tables 6−8 and plotted in Figures 4−6. Hydration numbers were calculated using the procedure described by Mohammadi et al.[37]

Figures 4−6 indicate a tendency similar to the hydrate dissociation curves reported for the CO_2 + H_2O system in Figure 3. This observed behavior indicates that the investigated

Table 5. Experimental Hydrate Dissociation Points (P and T) Measured in the Presence of CO_2 (Test System: CO_2 + H_2O) with Their Corresponding Enthalpies of Dissociation (ΔH_{diss}), Compressibility Factors (z), and Hydration Numbers (n)[a]

T_{exp} (K)	P_{exp} (MPa)	z (estimated)	ΔH_{diss} (kJ/mol CO_2)	n
282.3	3.8481	0.71	57.10	6.05
281.4	3.4222	0.75	60.24	6.08
280.4	2.9301	0.79	63.55	6.12
279.6	2.6281	0.82	65.44	6.15
278.8	2.3480	0.84	67.13	6.18
277.9	2.0493	0.86	68.88	6.22
276.8	1.7662	0.88	70.48	6.27
275.9	1.5963	0.89	71.40	6.29
274.7	1.4084	0.90	72.40	6.33
273.6	1.2861	0.91	73.03	6.35
272.6	1.1703	0.92	73.64	6.38

[a] $u(\Delta H)$ (0.95 level of confidence) ±1.5, $u(T)$ (0.95 level of confidence) ±0.08 K, $u(P)$ (0.95 level of confidence) ±0.0234 MPa.

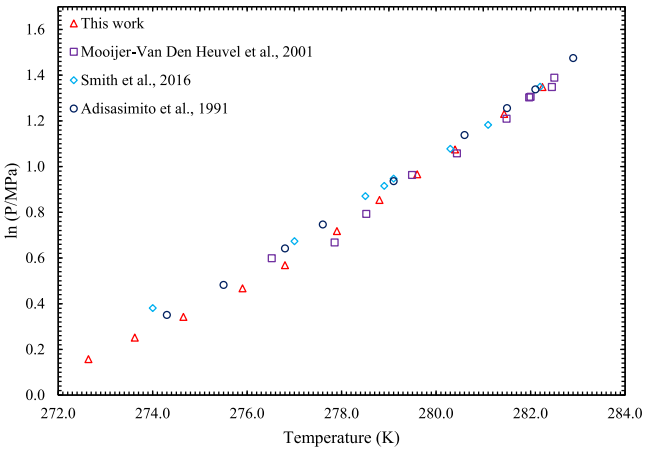

Figure 3. Experimental phase equilibrium data for carbon dioxide hydrate in pure water (system: CO_2 + H_2O). The literature data were taken from Mooijer et al.,[34] Smith et al.,[35] and Adisasmito et al.[36]

Table 6. Experimental Hydrate Dissociation Points (P and T) Measured in the Presence of CO_2 Hydrate Phase (System: CO_2 + Bitter Melon Juice + Water) with Their Corresponding Enthalpies of Dissociation (ΔH_{diss}), Compressibility Factors (z) and Hydration Numbers (n)[a]

W (wt %)	T_{exp} (K)	P_{exp} (MPa)	z (estimated)	ΔH_{diss} (kJ/mol CO_2)	n
96.5	280.8	4.5843	0.61	50.67	5.98
	280.4	4.1474	0.67	55.59	6.00
	279.8	3.7547	0.71	59.19	6.03
	279.0	3.3079	0.75	62.78	6.06
	278.2	2.9582	0.78	65.33	6.09
	277.1	2.5331	0.82	68.21	6.13
	275.8	2.1422	0.85	70.68	6.17
	274.5	1.8578	0.87	72.39	6.21
	273.0	1.5812	0.89	74.02	6.25
	272.1	1.4236	0.90	74.94	6.28
97.4	281.7	4.6334	0.61	50.44	5.98
	281.3	4.2456	0.66	54.80	6.01
	280.7	3.7612	0.71	59.20	6.04
	280.1	3.4163	0.75	61.91	6.06
	279.5	3.1404	0.77	63.92	6.08
	278.4	2.7041	0.81	66.89	6.12
	277.0	2.2490	0.84	69.78	6.17
	275.5	1.8977	0.87	71.88	6.21
	274.0	1.6016	0.89	73.60	6.26
	272.2	1.3099	0.91	75.27	6.32
98.3	282.5	4.7756	0.59	51.13	5.98
	282.1	4.3140	0.66	56.78	6.01
	281.7	3.9044	0.70	60.73	6.04
	281.1	3.5999	0.73	63.28	6.06
	280.6	3.3057	0.76	65.57	6.08
	279.7	2.9047	0.79	68.48	6.11
	279.0	2.6530	0.81	70.19	6.14
	278.1	2.3259	0.84	72.34	6.17
	277.0	2.0322	0.86	74.17	6.21
	275.5	1.7319	0.88	75.98	6.25
	273.3	1.3576	0.91	78.19	6.32

[a] $u(\Delta H)$ (0.95 level of confidence) ±1.5, $u(T)$ (0.95 level of confidence) ±0.08 K, $u(P)$ (0.95 level of confidence) ±0.0234 MPa, $u(W)$ (0.95 level of confidence) ±2.53 wt %.

https://doi.org/10.1021/acsomega.2c00551
ACS Omega 2022, 7, 34741−34751

Table 7. Experimental Dissociation Points (P and T) Measured in the Presence of CO_2 Hydrate Phase (System: CO_2 + Grape Juice + Water) with Their Corresponding Enthalpies of Dissociation (ΔH_{diss}), Compressibility Factors (z), and Hydration Numbers (n)[a]

W (wt %)	T_{exp} (K)	P_{exp} (MPa)	z (estimated)	ΔH_{diss} (kJ/mol CO_2)	n
88.5	281.9	4.7999	0.58	51.08	5.97
	281.2	4.3330	0.65	57.01	6.00
	280.5	3.9720	0.69	60.62	6.02
	280.0	3.7013	0.72	63.06	6.04
	279.5	3.4495	0.74	65.17	6.05
	278.9	3.1774	0.77	67.30	6.07
	278.2	2.8616	0.79	69.65	6.10
	277.1	2.4623	0.82	72.46	6.14
	275.8	2.0376	0.86	75.28	6.19
	274.5	1.7395	0.88	77.19	6.23
	273.6	1.5393	0.89	78.44	6.27
91.5	282.2	4.6578	0.61	55.24	5.98
	282.0	4.5427	0.63	56.69	5.99
	282.3	4.7097	0.60	54.52	5.98
	281.5	4.1858	0.67	60.69	6.01
	280.7	3.7402	0.72	64.94	6.04
	280.0	3.3875	0.75	67.94	6.07
	279.3	3.0655	0.78	70.48	6.09
	278.6	2.7433	0.80	72.89	6.12
	277.7	2.4016	0.83	75.31	6.16
	276.9	2.1479	0.85	77.03	6.19
	275.8	1.8336	0.87	79.11	6.23
	274.4	1.5457	0.89	80.95	6.28
	273.1	1.3264	0.91	82.32	6.33
94.3	282.9	4.5791	0.63	57.08	6.00
	282.4	4.2951	0.66	60.28	6.01
	281.8	3.9042	0.70	64.10	6.04
	281.2	3.5610	0.74	67.08	6.06
	279.8	2.9352	0.79	71.97	6.11
	278.4	2.4184	0.83	75.64	6.16
	276.4	1.8160	0.87	79.64	6.25
	274.5	1.4230	0.90	82.12	6.32

[a]$u(\Delta H)$ (0.95 level of confidence) ±1.5, $u(T)$ (0.95 level of confidence) ±0.08 K, $u(P)$ (0.95 level of confidence) ±0.0234 MPa, $u(W)$ (0.95 level of confidence) ±2.53 wt %.

Table 8. Experimental Dissociation Points (P and T) Measured in the Presence of CO_2 Hydrate Phase (System: CO_2 + Pineapple Juice + Water) with their Corresponding Enthalpies of Dissociation (ΔH_{diss}), Compressibility Factors (z), and Hydration Numbers (n)[a]

W (wt %)	T_{exp} (K)	P_{exp} (MPa)	z (estimated)	ΔH_{diss} (kJ/mol CO_2)	n
91.1	282.8	4.7549	0.60	48.82	5.98
	282.4	4.3944	0.65	52.93	6.01
	282.0	4.0779	0.69	55.90	6.03
	281.9	4.0222	0.69	56.39	6.03
	281.2	3.5931	0.73	59.85	6.06
	280.4	3.2004	0.77	62.69	6.09
	279.0	2.6532	0.81	66.31	6.14
	277.2	2.1019	0.85	69.66	6.20
	274.8	1.5786	0.89	72.65	6.28
	273.4	1.3594	0.91	73.86	6.32
	271.8	1.1779	0.92	74.83	6.36
93.3	281.9	4.5893	0.62	51.71	5.99
	281.5	4.2343	0.66	55.62	6.01
	280.9	3.8227	0.71	59.37	6.04
	279.7	3.2127	0.76	64.13	6.08
	278.8	2.7855	0.80	67.12	6.12
	277.0	2.2074	0.84	70.84	6.18
	274.9	1.7062	0.88	73.85	6.25
	273.4	1.4509	0.90	75.32	6.29
	272.2	1.2738	0.91	76.33	6.33
95.6	280.9	4.3425	0.64	55.29	5.99
	280.5	4.0110	0.68	58.70	6.02
	279.8	3.5830	0.73	62.47	6.05
	278.9	3.1157	0.77	66.12	6.08
	277.7	2.6094	0.81	69.69	6.13
	276.6	2.2511	0.84	72.05	6.16
	275.5	1.9521	0.86	73.96	6.20
	274.2	1.6515	0.88	75.80	6.25
	273.1	1.4604	0.90	76.93	6.28
	271.7	1.2493	0.91	78.17	6.33

[a]$u(\Delta H)$ (0.95 level of confidence) ±1.5, $u(T)$ (0.95 level of confidence) ±0.08 K, $u(P)$ (0.95 level of confidence) ±0.0234 MPa, $u(W)$ (0.95 level of confidence) = ± 2.53 wt %.

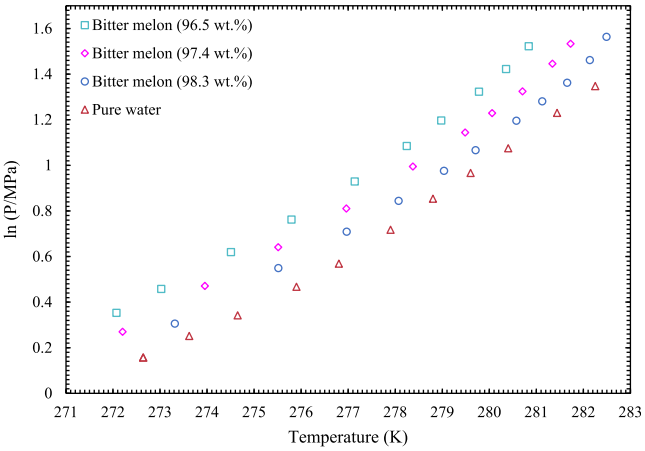

Figure 4. Experimental phase equilibrium data for carbon dioxide in bitter melon juice having less than 98.3 wt % of water cut.

juices' hydrate was only composed of pure water and carbon dioxide. Recycling and reusing materials (dissociated carbon dioxide and water) in the juice hydrate can reduce the energy costs associated with the subsequent separation processes. Solid particles dissolved in juice cannot be incorporated in the hydrate structure. However, they are likely to be trapped in its pores. Therefore, a treatment process may require reusing water to wash and clean the batch-hydrate crystallizer equipment when the gas has been released from water molecules. Also, recycled water may be used to dilute cleaning agents to a proper concentration. This water may also be utilized to clean and disinfect the process equipment involved in fruit juice production. This would reduce the costs of utilities required for cleaning. Despite the requirements of the treatment process, according to the thermodynamic conditions for the process, it is evident that the hydrate-based technology may be applied as an alternative to existing commercial technologies for aqueous solution concentration. However, it is noteworthy that before this technology can be used one will be required to perform a feasibility study that also includes kinetics and transport phenomena associated with hydrate formation.

https://doi.org/10.1021/acsomega.2c00551
ACS Omega 2022, 7, 34741−34751

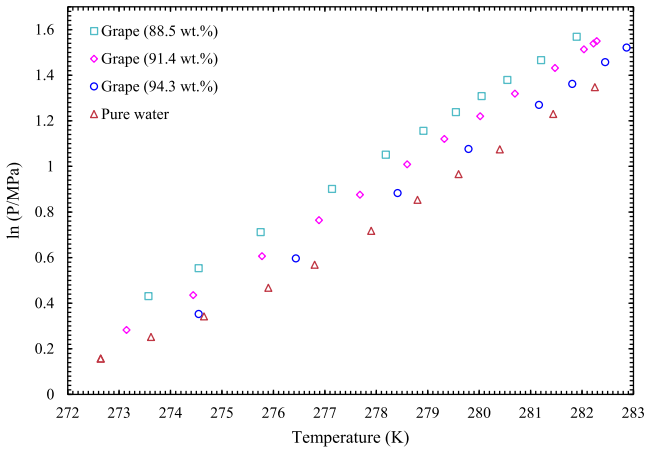

Figure 5. Experimental phase equilibrium data for carbon dioxide hydrate in grape fruit juice having less than 94.3 wt % of water cut.

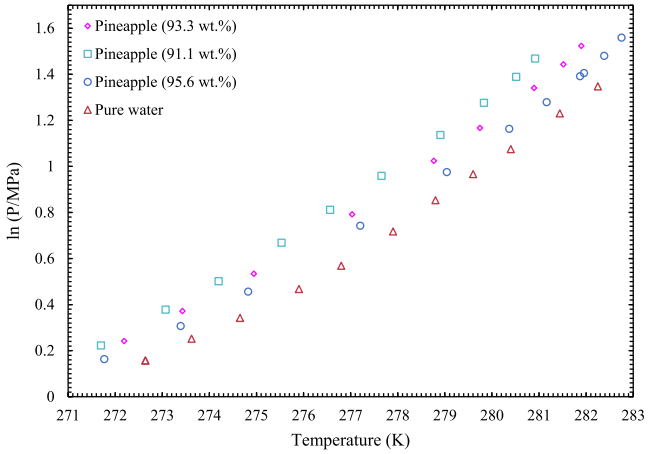

Figure 6. Experimental phase equilibrium data for carbon dioxide hydrate in pineapple fruit juice having less than 95.6 wt % of water cut.

The obtained hydrate dissociation points for all three systems revealed that a slight increase in the dissociation temperature results in a drastic increase in the dissociation pressure. The possibility of obtaining erroneous values for the measured hydrate dissociation conditions was prevented by prolonged and careful adjustments. For this reason, during the heating phase, the system temperature was increased stepwise by 0.1 K/h until the equilibrium dissociation point was obtained. Moreover, it is advisible to consider systems with moderate or low pressures to minimize the compression costs.

Conversely, on the basis of the obtained results, it is expected that high energy requirements may be necessary for concentrating the investigated juices through hydrate formation at pressures as high as those reported in this study. This may be avoided by injecting a water-soluble material referred to as a promoter to lower the system pressure.

It was revealed that system pressures below 2.0 MPa might require the addition of a water-insoluble hydrate inhibitor to avoid ice formation for temperatures close to or below 273.15 K. This is the lowest pressure for the hydrate dissociation pressure of carbon dioxide under $H-L-V$ equilibrium conditions. The experimentally observed high hydrate dissociation pressures have been attributed to dissolved solids in fruit juices, disrupting the encapsulation of carbon dioxide gas into water cavities. Further phase behavior studies are required at dissociation temperatures higher than those reported in this study. This could assist in a better examination of the dependence of the dissociation pressures on the water content in the investigated systems.

3.1.1. Influence of Dissolved Solids in Hydrate Phase Equilibrium Data. CO_2 hydrate dissociation data were obtained in the present study in the temperature range of 271.7−282.8 K and pressures range of 1.25−4.79 MPa, suitable for fruit juice preservation. Dissociation data presented by Figures 4−6 indicate some interesting findings. It is observed that all investigated juices were able to slightly shift CO_2 hydrate dissociation curves toward lower temperature (by 1.5 K on average for pure juice) and higher pressure zones. This observed behavior confirms that interactions between the constituents of investigated juices and water lead to inhibiting effects. These substantial inhibiting effects are similar to those of alcohols, glycols, and electrolytes reported in the literature.[38−40]

Understanding the inhibitory effects of the investigated fruit juices on hydrate formation is essential for process development purposes. It is well-known that hydrate dissociation conditions are highly dependent on the physical properties of the investigated juices and those of carbon dioxide. Since juice constituents have either hydroxyl groups or large molecules, their size and chemical nature do not allow them to be part of the hydrate structure. Therefore, these inhibiting effects could be due to the combination of strong hydrogen bonds formed by dissolved juice constituents which interact electrostatically with the other water molecules.

According to the literature, polymers, sugars, essential minerals, and organic acids inhibit hydrate formation thermodynamically and kinetically. Therefore, residuals (soluble solids) such as natural polymers (pectin), proteins, and sugars (i.e., fructose and glucose) were the main contributors to these inhibiting effects. Sugars (fructose and glucose) contain four hydroxyl groups and one carbonyl group in their structure, forming strong hydrogen bonds with water molecules. The dissociation conditions for new systems reported in the present study and those for the CO_2 + sucrose/fructose/glucose model solution system are in the same range.[20,21,41] Therefore, since they are present in tremendous amounts in juices, sugars strongly influenced hydrate formation in the investigated systems.

The fruit juice pH and system temperature played a decisive role in influencing the competition between sugars and lipid chains contained in juices. The pH scale of all investigated juices was below 4.6. Sugars at this pH scale are known to exhibit higher chemical stability. Since at this pH scale fermentation may not take place, the observed inhibiting effects could not be attributed to the presence of alcohols. The minerals present could not participate in hydrate formation but dissociate to cations and anions, decreasing the fruit juice's water activity. This is because the inhibition mechanism of combined inhibitors reduces molecular activities, thus increasing the competition for water molecules. These constituents instigated the intermolecular interactions with carbon dioxide to increase the system's acidity. Constituents disrupt the hydrogen bonds of host water molecules that build up the cage frameworks of the hydrate structure. On the basis of the results presented in plots, it can be deduced that the constituents present in bitter melon fruit juice have a higher inhibiting strength in comparison to those in grape and

https://doi.org/10.1021/acsomega.2c00551
ACS Omega 2022, 7, 34741−34751

pineapple fruit juices. Observations made in this study illustrate the necessity of undertaking hydrate-based concentration studies on freshly extracted juices rather than commercial juices sold in supermarkets, as the constituents are better known in the latter than in the former juices.

3.1.2. Influence of Water Cut on Hydrate Phase Equilibrium Data. The water content of the investigated systems is of great interest in designing carbon dioxide hydrate based fruit juice concentration processes. The investigated juices had a water cut ranging from 88.5 to 96.5 wt %. The shift in hydrate dissociation conditions was reduced by increasing the juice water content. The effects of water addition on carbon dioxide hydrate inhibition were almost identical at all investigated juice concentrations. It can be observed that freshly extracted fruit juices (88.5, 91.1, and 96.5 wt % of water) had higher inhibitory effects than juices at 91.4, 93.3, 94.3, 95.6, 97.4, and 98.3 wt % of water. The inhibition effects of fruit juice components on carbon dioxide hydrates decreased as the contents' concentration was decreased due to Millipore water addition. Therefore, it is proposed that economic studies be undertaken to obtain the optimal quantity of water in fruit juice for an effective hydrate-based concentration. Furthermore, it is suggested that further studies validate this hypothesis. Additionally, the strength of relevant juice constituents should be determined, as this information is crucial for developing thermodynamic models.

It can also be highlighted that hydrate dissociation curves of carbon dioxide of the three juices investigated in this study have a inhibitory tendency similar to those reported in the literature[14,17,27−29] for other juices. However, inhibition effects observed in this study were slightly higher than those of previously investigated juices. Li et al.[27] indicated that orange juice had a slight effect on the hydrate dissociation conditions of carbon dioxide. Therefore, the authors successfully regressed the obtained experimental data by ignoring the inhibitory effects of juice contents on hydrate dissociation. Conversely, in this study, the observed inhibitory effects were significant. Therefore, these effects may not be ignored when a predictive thermodynamic model is developed to calculate the dissociation points for the investigated systems. Thermodynamic calculations can determine the dependence of macroscopic and microscopic properties on system pressure and temperature to understand this behavior better. This information would greatly interest the industry with regard to the process design/optimization of the newly proposed fruit juice concentration process.

3.1.3. Assessment of Temperature Dependence. This study used experimental dissociation points to assess the thermal properties by predicting and estimating the heat required to dissociate carbon dioxide hydrates in the presence of juices. Hydrate dissociation is an endothermic process, since it requires energy to break the hydrate crystals. Therefore, this process reflects the hydrate stability, crystal hydrogen bonding, and cavity occupation. Thus, considering the thermal properties is essential for the design/optimization of the new carbon dioxide hydrate based fruit juice concentration process. In the present study, molar dissociation enthalpies of carbon dioxide hydrates in the test system and new systems were estimated using the experimental hydrate dissociation data and the Clausius−Clapeyron equation (1). Gas compression was taken into account by calculating the compressibility factor for each corresponding hydrate dissociation point reported in this study.

$$\Delta H = -zR\left(\frac{\mathrm{d}\ln P}{\mathrm{d}\left(\frac{1}{T}\right)}\right) \quad (1)$$

In eq 1, P and T are the hydrate dissociation pressure and temperature of carbon dioxide, respectively, ΔH_{diss} is the molar enthalpy of dissociation, R is the universal gas constant, and z is the compressibility factor of the carbon dioxide gas, which is calculated using the Soave−Redlich−Kwong (SRK) equation of state.[42] In this equation, the ratio $\mathrm{d}\ln P/\mathrm{d}(1/T)$ is the slope of the line produced by plotting $\ln P$ against $1/T$. It is calculated by using the hydrate dissociation points reported in Tables 6−8 and Figures 4−6. This equation can be used to calculate ΔH_{diss} when z does not change significantly over the range of the measured hydrate dissociation points, and it is valid for univariant systems. Furthermore, ΔH_{diss} must not change significantly over a narrow temperature range.

The graphical representations of molar hydrate dissociation enthalpy are presented in Figures 7−9. The semilogarithmic plot ($\ln P$ vs $1/T$) shows a linear relationship that validates the Clausius−Clapeyron equation for the considered range of

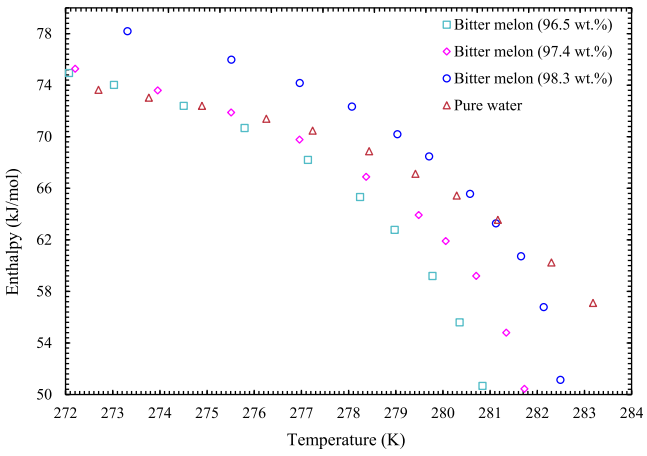

Figure 7. Predicted molar enthalpy corresponding to the experimental hydrate dissociation conditions for carbon dioxide in the presence and absence of bitter melon juice having less than 98.3 wt % of water cut.

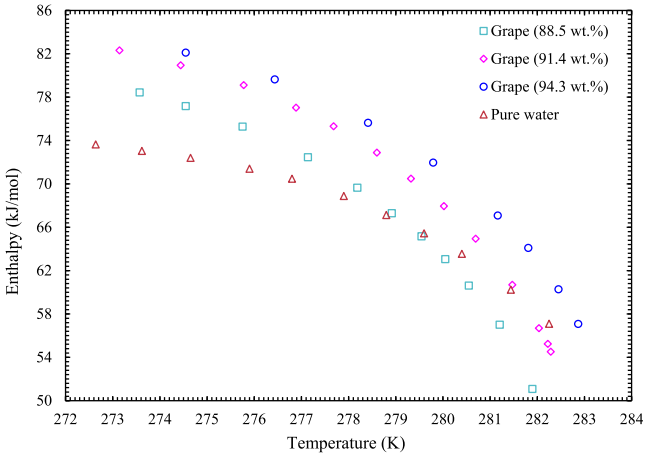

Figure 8. Predicted molar enthalpy corresponding to the measured hydrate dissociation conditions for carbon dioxide in the presence and absence of grape juice having less than 94.3 wt % of water cut.

https://doi.org/10.1021/acsomega.2c00551
ACS Omega 2022, 7, 34741−34751

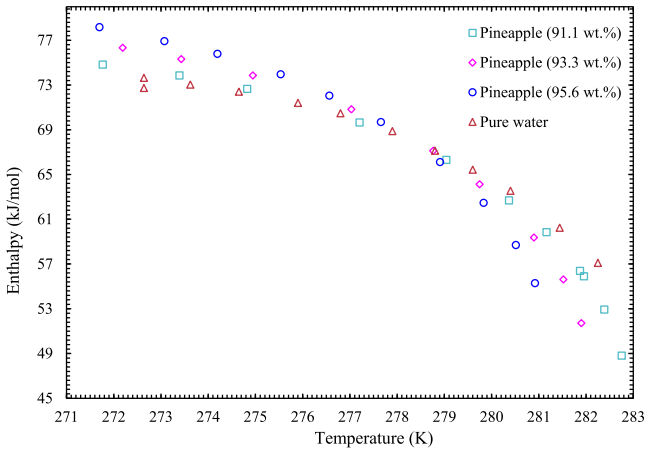

Figure 9. Predicted molar enthalpy corresponding to the measured hydrate dissociation conditions for carbon dioxide in the presence and absence of pineapple juice having less than 95.6 wt % of water cut.

experimental hydrate dissociation data. The values of compressibility factors were obtained by assuming that carbon dioxide is immiscible in water and that the amount of water in the vapor phase is negligible. The obtained ΔH_{diss} values indicate a strong relationship with z, and both properties change in the same order of magnitude. This observed behavior supports the claims made by Skovborg and Rasmussen[43] that, for the univariant slope of the phase equilibrium boundary (ln P vs $1/T$) to be constant, these values must display the same order of magnitude.

It can be seen that the enthalpies of carbon dioxide hydrate dissociation in each investigated system and the $CO_2 + H_2O$ system indicate an exponential temperature dependence. Notably, the hydrate dissociation conditions are set by the type of hydrate structure and guest molecules. Therefore, the hydrate dissociation points indicated a dependence on the guest molecule size and cavity size ratio. The average hydrate dissociation enthalpy for the $CO_2 + H_2O$ system was found to be 67.66 ± 1.5 kJ/mol of CO_2 for a temperature range of 272.6−282.2 K. The hydrate dissociation enthalpy values varied in the order CO_2 + grape > CO_2 + pineapple > CO_2 + bitter melon, while the corresponding average values were 67.83 ± 1.5, 64.19 ± 1.5, and 63.44 ± 1.5 kJ/mol of CO_2, respectively. There are few deviations between the investigated systems and the test system. Furthermore, these were compared to reported data on dissociation enthalpies of CO_2 hydrates in pure water or fruit juice. The dissociation enthalpies of new systems and those calculated in the literature are in the same range.

A reason for the preservation of valuable juice components is the hydrate structure itself. It is assumed that an sI hydrate is formed for the systems investigated as only CO_2 gas is available,[44] and inhibitors participated by preventing gas hydrate formation. It is observed that the values of ΔH_{diss} for new systems are slightly higher in comparison to those of the test systems. As shown in Tables 6−8, the observed behavior indicates that inhibitors do not change or affect the hydrate structure. Sloan and Fleyfel[45] pointed out that the dissociation enthalpy of a gas hydrate primarily depends on the hydrate structure and cage occupancy of guest molecules, and 80% of the enthalpy is due to the strength of water hydrogen bonds in the hydrate structure. Therefore, as long as the same hydrate structure is formed, ΔH_{diss} will be the same.

In the present study, the observed slight increases in the values of ΔH_{diss} may be attributed to slight increases in the interactions between the hydrate lattice and CO_2 molecules. This signifies that higher pressures and lower temperatures are required to form hydrates. The increase in the hydrate dissociation enthalpy is an indication that the hydrate phase is approaching a more stable region.

4. CONCLUSION

In this work, the hydrate phase equilibrium data of new systems (system 1, CO_2 + grape; system 2, CO_2 + pineapple; system 3, CO_2 + bitter melon) were studied under different water cuts of fruit juice solutions. It was observed that the investigated juices considerably shifted the CO_2 phase equilibrium curve to higher pressures and lower temperatures. This increased with a reduction in juice water cuts while the observed inhibitory effects were significant. These effects may not be ignored when predictive thermodynamic models are developed to calculate the dissociation points for the investigated systems. The obtained results also suggest that it is advisible to undertake experiments and modeling studies on fresh juices rather than commercial (supermarket) juices containing some additives.

AUTHOR INFORMATION

Corresponding Author

Kaniki Tumba − *Department of Chemical Engineering, Thermodynamics, Materials and Separations Research Group (TMSRG), Mangosuthu University of Technology, Durban 4031, South Africa;* orcid.org/0000-0003-2685-3741; Email: tumba@mut.ac.za

Authors

Nkululeko Nkosi − *School of Chemical and Metallurgical Engineering, Oil and Gas Production and Processing Research Unit, University of the Witwatersrand, Johannesburg 2001, South Africa; Department of Chemical Engineering, Thermodynamics, Materials and Separations Research Group (TMSRG), Mangosuthu University of Technology, Durban 4031, South Africa;* orcid.org/0000-0002-9151-3359

Diakanua Nkazi − *School of Chemical and Metallurgical Engineering, Oil and Gas Production and Processing Research Unit, University of the Witwatersrand, Johannesburg 2001, South Africa;* orcid.org/0000-0001-8143-705X

Complete contact information is available at: https://pubs.acs.org/10.1021/acsomega.2c00551

Notes

The authors declare no competing financial interest.

ACKNOWLEDGMENTS

This study was supported by the Mangosuthu University of Technology and Witwatersrand University. N.N. wishes to thank the Council for Scientific and Industrial Research (CSIR) in South Africa for financial support while undertaking this research project.

REFERENCES

(1) Hwang, C. C.; Tour, J. J.; Kittrell, C.; Espinal, L.; Alemany, L. B.; Tour, J. M. Capturing Carbon Dioxide as a Polymer from Natural Gas. *Nature Communications.* **2014**, *5*, 3961.

(2) van Soest, H. L.; den Elzen, M. G. J.; van Vuuren, D. P. Net-Zero Emission Targets for Major Emitting Countries Consistent with the Paris Agreement. *Nat. Commun.* **2021**, *12* (1), 2140.
(3) Charani Shandiz, S.; Rismanchi, B.; Foliente, G. Energy Master Planning for Net-Zero Emission Communities: State of the Art and Research Challenges. *Renew. Sustain. Energy Rev.* **2021**, *137*, 110600.
(4) Lützkendorf, T.; Balouktsi, M. On Net Zero GHG Emission Targets for Climate Protection in Cities: More Questions than Answers? *IOP Conf. Ser. Earth Environ. Sci.* **2019**, *323* (1), 012073.
(5) Makogon, Y. F. Natural Gas Hydrates - A Promising Source of Energy. *J. Nat. Gas Sci. Eng.* **2010**, *2* (1), 49−59.
(6) Chong, Z. R.; He, T.; Babu, P.; Zheng, J.-n.; Linga, P. Economic Evaluation of Energy Efficient Hydrate Based Desalination Utilizing Cold Energy from Liquefied Natural Gas (LNG). *Desalination* **2019**, *463*, 69−80.
(7) Ong, C. W.; Chen, C. L. Technical and Economic Evaluation of Seawater Freezing Desalination Using Liquefied Natural Gas. *Energy* **2019**, *181*, 429−439.
(8) Ngema, P. T.; Naidoo, P.; Mohammadi, A. H.; Ramjugernath, D. Phase Stability Conditions for Clathrate Hydrates Formation in CO2 + (NaCl or CaCl2 or MgCl2) + Cyclopentane + Water Systems: Experimental Measurements and Thermodynamic Modeling. *J. Chem. Eng. Data* **2019**, *64* (11), 4638−4646.
(9) Tumba, K.; Babaee, S.; Naidoo, P.; Mohammadi, A. H.; Ramjugernath, D. Phase Equilibria of Clathrate Hydrates of Ethyne + Propane. *J. Chem. Eng. Data* **2014**, *59* (9), 2914−2919.
(10) Sergeeva, M. S.; Mokhnachev, N. A.; Shablykin, D. N.; Vorotyntsev, A. V.; Zarubin, D. M.; Atlaskin, A. A.; Trubyanov, M. M.; Vorotyntsev, I. V.; Vorotyntsev, V. M.; Petukhov, A. N. Xenon Recovery from Natural Gas by Hybrid Method Based on Gas Hydrate Crystallisation and Membrane Gas Separation. *J. Nat. Gas Sci. Eng.* **2021**, *86*, 103740.
(11) Gambelli, A. M.; Castellani, B.; Nicolini, A.; Rossi, F. Gas Hydrate Formation as a Strategy for CH4/CO2 Separation: Experimental Study on Gaseous Mixtures Produced via Sabatier Reaction. *J. Nat. Gas Sci. Eng.* **2019**, *71*, 102985.
(12) Tan, L. S.; Shariff, A. M.; Lau, K. K.; Bustam, M. A. Impact of High Pressure on High Concentration Carbon Dioxide Capture from Natural Gas by Monoethanolamine/N-Methyl-2-Pyrrolidone Solvent in Absorption Packed Column. *Int. J. Greenh. Gas Control* **2015**, *34*, 25−30.
(13) Wilberforce, T.; Olabi, A. G.; Sayed, E. T.; Elsaid, K.; Abdelkareem, M. A. Progress in Carbon Capture Technologies. *Sci. Total Environ.* **2021**, *761*, 143203.
(14) Li, S.; Shen, Y.; Liu, D.; Fan, L.; Tan, Z. Concentrating Orange Juice through CO2 Clathrate Hydrate Technology. *Chem. Eng. Res. Des.* **2015**, *93* (July), 773−778.
(15) Huang, C. P.; Fennema, O.; Powrie, W. D. Gas Hydrates in Aqueous-Organic Systems: II. Concentration by Gas Hydrate Formation. *Cryobiology* **1966**, *2* (5), 240−245.
(16) Ngan, Y. T.; Englezos, P. Concentration of Mechanical Pulp Mill Effluents and NaCl Solutions through Propane Hydrate Formation. *Ind. Eng. Chem. Res.* **1996**, *35* (6), 1894−1900.
(17) Li, S.; Shen, Y.; Liu, D.; Fan, L.; Tan, Z.; Zhang, Z.; Li, W.; Li, W. Experimental Study of Concentration of Tomato Juice by CO2 Hydrate Formation. *Chem. Ind. Chem. Eng. Q.* **2015**, *21* (3), 441−446.
(18) Safari, S.; Varaminian, F. Study the Kinetics and Thermodynamics Conditions for CO2 Hydrate Formation in Orange Juice Concentration. *Innov. Food Sci. Emerg. Technol.* **2019**, *57*, 102155.
(19) Ghiasi, M. M.; Mohammadi, A. H.; Zendehboudi, S. Clathrate Hydrate Based Approach for Concentration of Sugar Aqueous Solution, Orange Juice, and Tomato Juice: Phase Equilibrium Modeling Using a Thermodynamic Framework. *Fluid Phase Equilib.* **2020**, *512*, 112460.
(20) Andersen, T. B.; Thomsen, K. Separation of Water through Gas Hydrate Formation. *Int. Sugar J.* **2009**, *111* (1330), 632−636.
(21) Doubra, P.; Hassanalizadeh, R.; Naidoo, P.; Ramjugernath, D. Thermodynamic Measurement and Modeling of Hydrate Dissociation for CO2/Refrigerant + Sucrose/Fructose/Glucose Solutions. *AIChE J.* **2021**, *67*, 1−11.
(22) Srivastava, S.; Hitzmann, B.; Zettel, V. A Future Road Map for Carbon Dioxide (CO2) Gas Hydrate as an Emerging Technology in Food Research. *Food Bioprocess Technol.* **2021**, *14* (9), 1758−1762.
(23) Wang, X.; Zhang, F.; Lipiński, W. Carbon Dioxide Hydrates for Cold Thermal Energy Storage: A Review. *Sol. Energy* **2020**, *211*, 11−30.
(24) Claßen, T.; Seidl, P.; Loekman, S.; Gatternig, B.; Rauh, C.; Delgado, A. Review on the Food Technological Potentials of Gas Hydrate Technology. *Curr. Opin. Food Sci.* **2019**, *29*, 48−55.
(25) Abedi-Farizhendi, S.; Hosseini, M.; Iranshahi, M.; Mohammadi, A.; Manteghian, M.; Mohammadi, A. H. Kinetics of CO 2 Hydrate Formation in Coffee Aqueous Solution: Application in Coffee Concentration. *J. Dispers. Sci. Technol.* **2020**, *41* (6), 895−901.
(26) Purwanto, Y. A.; Oshita, S.; Seo, Y.; Kawagoe, Y. Concentration of Liquid Foods by the Use of Gas Hydrate. *J. Food Eng.* **2001**, *47* (2), 133−138.
(27) Li, S.; Shen, Y.; Liu, D.; Fan, L.; Zhang, Z.; Li, W.; Tan, Z.; Li, W.; Bai, J. Measurement and Prediction of Hydrate Phase Equilibrium of Orange Juice + CO2, C2H4 or C2H6 for Orange Juice Concentration. *Adv. J. Food Sci. Technol.* **2016**, *10* (12), 890−893.
(28) Claßen, T.; Jaeger, M.; Loekman, S.; Gatternig, B.; Rauh, C.; Delgado, A. Concentration of Apple Juice Using CO2 Gas Hydrate Technology to Higher Sugar Contents. *Innov. Food Sci. Emerg. Technol.* **2020**, *65*, 102458.
(29) Seidl, P.; Loekman, S.; Sardogan, M.; Voigt, E.; Claßen, T.; Ha, J.; Luzi, G.; Sevenich, R.; Agudo, J. R.; Rauh, C.; Delgado, A. Food Technological Potentials of CO 2 Gas Hydrate Technology for the Concentration of Selected Juices. *High Press. Res.* **2019**, *39* (2), 344−356.
(30) AOAC International. *Official Methods of Analysis of AOAC International*, 20th ed.; AOAC: 2016.
(31) Sloan, E. D.; Koh, C. A. *Clathrate Hydrates of Natural Gases*; Chemical Industries; CRC Press: 2007; Vol. *20074156*. DOI: 10.1201/9781420008494.
(32) Tumba, K.; Reddy, P.; Naidoo, P.; Ramjugernath, D.; Eslamimanesh, A.; Mohammadi, A. H.; Richon, D. Phase Equilibria of Methane and Carbon Dioxide Clathrate Hydrates in the Presence of Aqueous Solutions of Tributylmethylphosphonium Methylsulfate Ionic Liquid. *J. Chem. Eng. Data* **2011**, *56* (9), 3620−3629.
(33) Carroll, J. *Natural Gas Hydrates - A Guide for Engineers*, 3rd ed.; Gulf Professional Publications/Elsevier: 2014.
(34) Mooijer-Van Den Heuvel, M. M.; Witteman, R.; Peters, C. J. Phase Behaviour of Gas Hydrates of Carbon Dioxide in the Presence of Tetrahydropyran, Cyclobutanone, Cyclohexane and Methylcyclohexane. *Fluid Phase Equilib.* **2001**, *182* (1−2), 97−110.
(35) Smith, A.; Babaee, S.; Mohammadi, A. H.; Naidoo, P.; Ramjugernath, D. Clathrate Hydrate Dissociation Conditions for Refrigerant + Sucrose Aqueous Solution: Experimental Measurement and Thermodynamic Modelling. *Fluid Phase Equilib.* **2016**, *413*, 99−109.
(36) Adisasmito, S.; Frank, R. J.; Sloan, E. D. Hydrates of Carbon Dioxide and Methane Mixtures. *J. Chem. Eng. Data* **1991**, *36* (1), 68−71.
(37) Mohammadi, A.; Manteghian, M.; Haghtalab, A.; Mohammadi, A. H.; Rahmati-Abkenar, M. Kinetic study of carbon dioxide hydrate formation in presence of silver nanoparticles and SDS. *Chem. Eng. J.* **2014**, *237*, 387−395.
(38) Saberi, A.; Alamdari, A.; Shariati, A.; Mohammadi, A. H. Experimental Measurement and Thermodynamic Modeling of Equilibrium Condition for Natural Gas Hydrate in MEG Aqueous Solution. *Fluid Phase Equilib.* **2018**, *459*, 110−118.
(39) Burgass, R.; Chapoy, A.; Li, X. Gas Hydrate Equilibria in the Presence of Monoethylene Glycol, Sodium Chloride and Sodium Bromide at Pressures up to 150 MPa. *J. Chem. Thermodyn.* **2018**, *118*, 193−197.

https://doi.org/10.1021/acsomega.2c00551
ACS Omega 2022, 7, 34741−34751

(40) Nasir, Q.; Suleman, H.; Elsheikh, Y. A. A Review on the Role and Impact of Various Additives as Promoters/ Inhibitors for Gas Hydrate Formation. *J. Nat. Gas Sci. Eng.* **2020**, *76*, 103211.
(41) Chun, M. K.; Lee, H. Phase Equilibria of Carbon Dioxide Hydrate System in the Presence of Sucrose, Glucose, and Fructose. *J. Chem. Eng. Data* **1999**, *44* (5), 1081−1084.
(42) Soave, G. Equilibrium Constants from a Modified Redkh-Kwong Equation of State. *Chem. Eng. Sci.* **1972**, *27*, 1197−1203.
(43) Skovborg, P.; Rasmussen, P. Comments on: Hydrate Dissociation Enthalpy and Guest Size. *Fluid Phase Equilib.* **1994**, *96* (C), 223−231.
(44) Lee, H. J.; Lee, J. D.; Linga, P.; Englezos, P.; Kim, Y. S.; Lee, M. S.; Kim, Y. Do. *Gas Hydrate Formation Process for Pre-Combustion Capture of Carbon Dioxide* **2010**, *35*, 2729.
(45) Sloan, E. D.; Fleyfel, F. Reply to "Comments on: Hydrate Dissociation Enthalpy and Guest Size. *Fluid Phase Equilib.* **1994**, *96* (C), 233−235.

https://doi.org/10.1021/acsomega.2c00551
ACS Omega 2022, 7, 34741−34751